Supporting Information

Magnetic field assisted self-assembly strategy towards strongly coupled Fe_3O_4 nanocrystals/rGO paper for high-performance lithium ion batteries

By *Kan Zhang[†], Wei Zhao[§], Jeong-Taik Lee[†], Geewoo Chang[†], Xinjian Shi[‡], Jong Hyeok Park[†‡*]*

[*]K. Zhang, J. T. Lee, Geewoo Jang, Prof. J. H. Park*
SKKU Advanced Institute of Nanotechnology (SAINT), Sungkyunkwan University, Suwon 440-746, Republic of Korea Fax: (+ 82) 31-290-7346,
Lutts@skku.edu.
X. J. Shi, Prof. J. H. Park
School of Chemical Engineering, Sungkyunkwan University, Suwon 440-746, Republic of Korea Fax: (+ 82) 31-290-7346,
Dr. W. Zhao
School of Materials Science and Engineering, Yeungnam University, Gyeongsan, Gyeongbuk 712-749, Republic of Korea

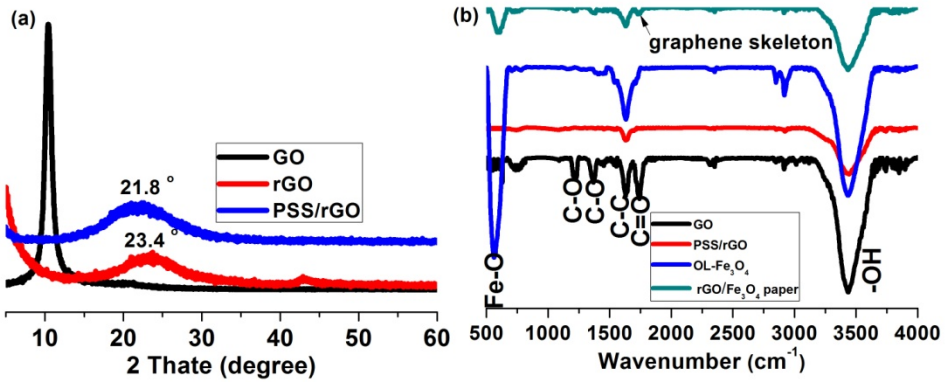

Figure S1. (a) XRD patterns of GO, rGO and PSS/rGO; (b) FT-IR spectra of GO, PSS/rGO, OL-Fe_3O_4 and rGO/Fe_3O_4.

The interlayer spacing of GO, rGO and PSS/rGO can be roughly calculated by Bragg equation:
$d_{002}=\lambda/2\sin\theta$
where λ is 1.54 Å
Results showed the the interlayer spacing of PSS/rGO is larger than that of rGO, indicating strong electrostatic repulsion between layer and layer in PSS/rGO.

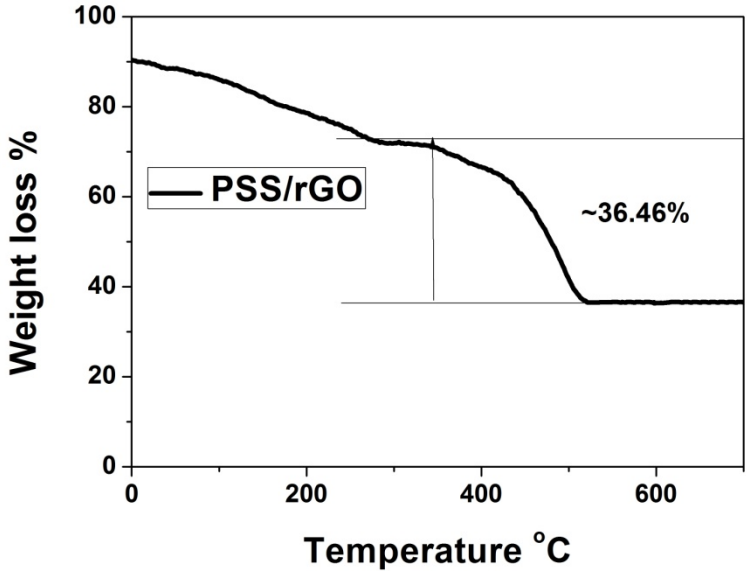

Figure S2. TGA analysis of PSS/rGO in N_2 atmosphere with heated at a rate of 1°C/min.

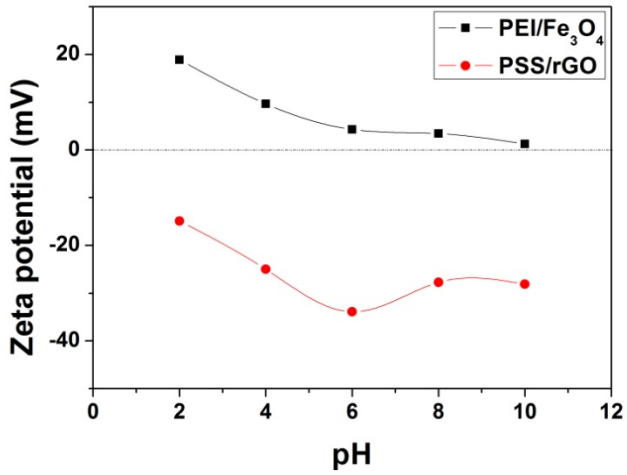

Figure S3. pH-dependent ζ-potential of PEI/Fe_3O_4 and PSS/rGO suspensions.

Figure S4. Digital picture of PSS/rGO paper.

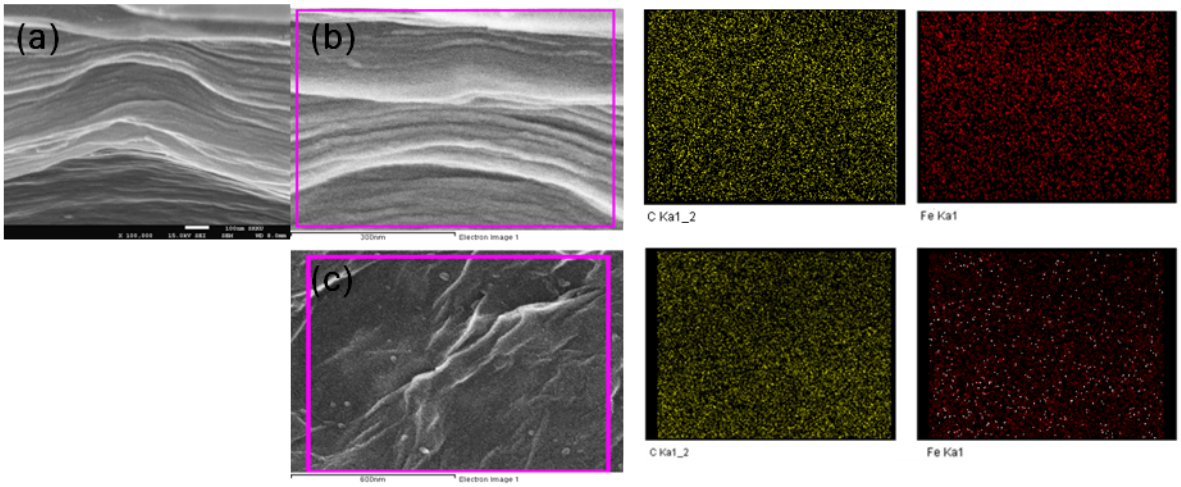

Figure S5. Section and top view of rGO/Fe_3O_4 hybrid paper.

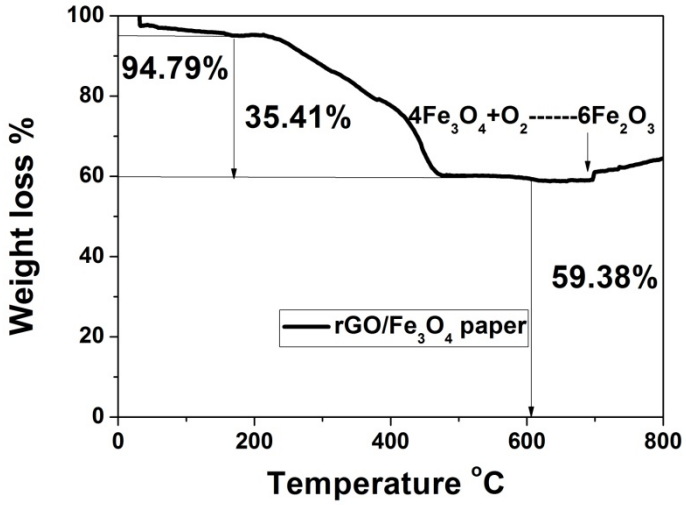

Figure S6. TGA analysis of rGO/Fe_3O_4 hybrid paper in air atmosphere with heated at a rate of 1°C/min.

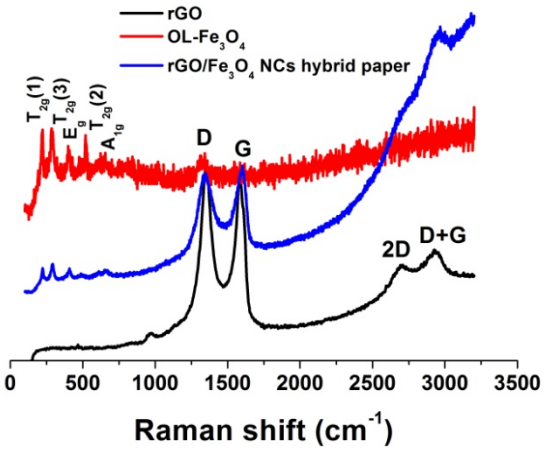

Figure S7. Raman shift of rGO, OL-Fe_3O_4 and rGO/Fe_3O_4 NCs hybrid paper.

Five Raman active modes at 193 cm^{-1} [$T_{2g}(1)$], 306 cm^{-1} [$T_{2g}(3)$], 408 cm^{-1} (E_g), 542 cm^{-1} [$T_{2g}(2)$] and 669 cm^{-1} (A_{1g}) in OL-Fe_3O_4 and rGO/Fe_3O_4 NCs hybrid paper are consistent with cubic Fe_3O_4. [S1]

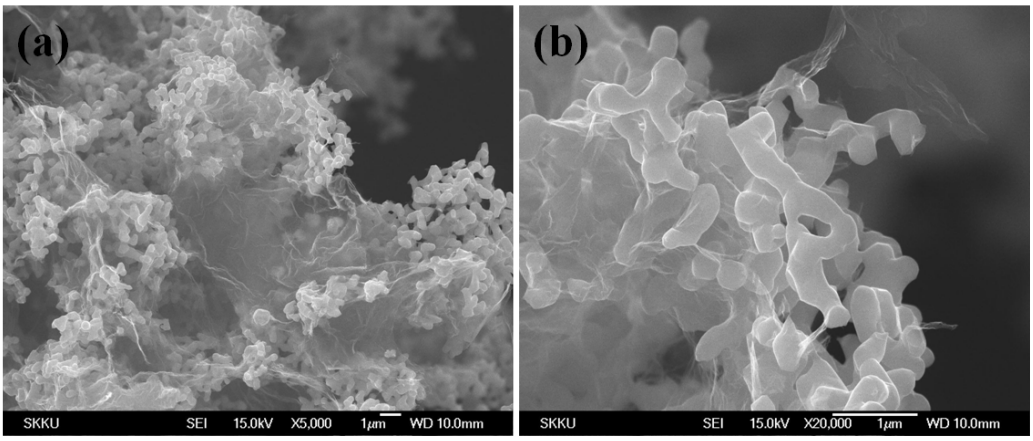

Figure S8. SEM images of powdered rGO/Fe_3O_4.

The size distribution is about 200-400 nm.

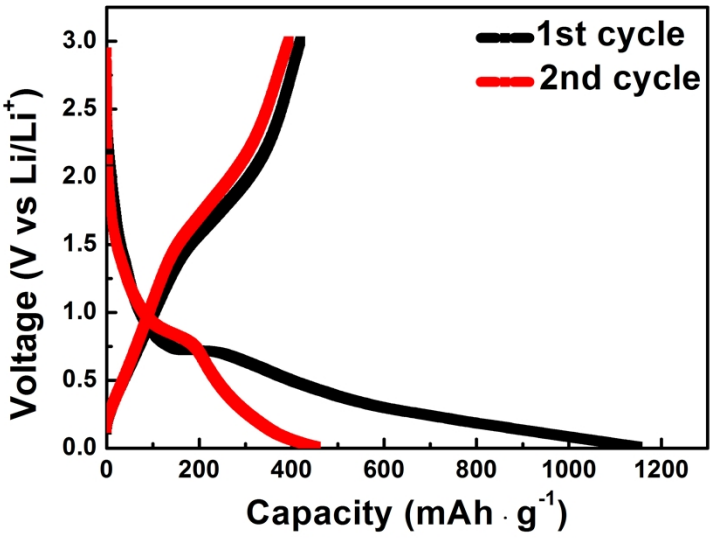

Figure S9. Charge-discharge voltage profiles at current density of 1C of self-assembly rGO/Fe_3O_4.

In the cases of the self-assembly rGO/Fe_3O_4 hybrid paper, the first discharge curves showed a prominent potential plateau at about 0.75V versus Li^+/Li. However, the potential plateau in self-assembly rGO/Fe_3O_4 hybrid paper was very short compared to its capacity, which suggested a less conversion reaction and dominant electrolyte decomposition and/or other side reactions. The phenomenon might be ascribed to poor ionic and electrical conductivity in presence of PSS and PEI ployelectrolyte.

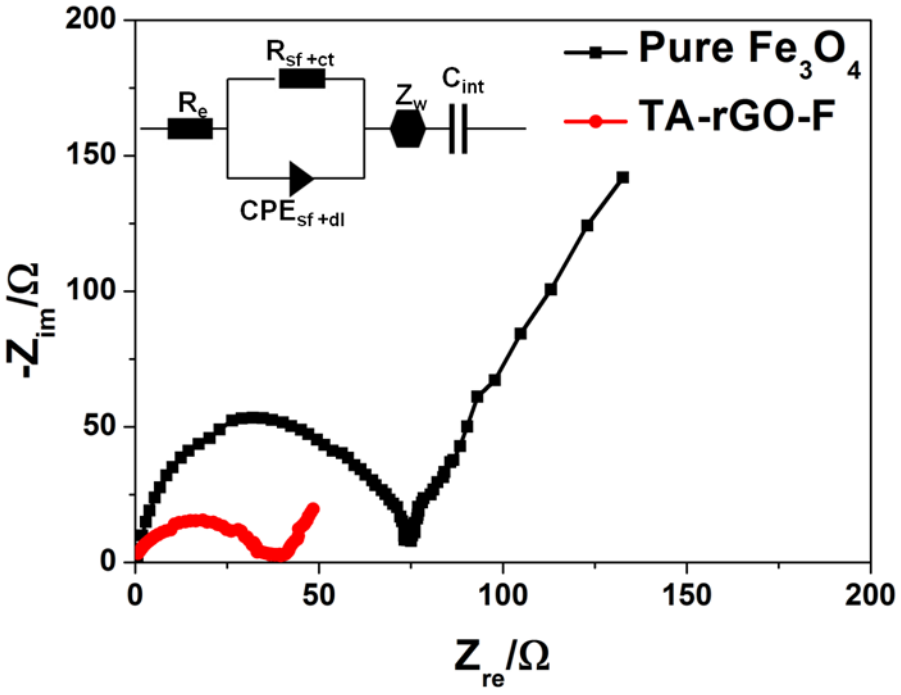

Figure S10. Nyquist plots of the pure Fe_3O_4 and rGO/Fe_3O_4 NCs hybrid paper obtained after the 3 cycles by applying a sine wave with amplitude of 5.0 mV over the frequency range from 100 kHz to 0.01 Hz, and inset is the equivalent electrical circuit.

The elements in the equivalent circuit include ohmic resistance of the electrolyte and cell components (R_e), surface film resistance (R_{sf}), charge-transfer resistance at the interface between the electrode and electrolyte (R_{ct}), a constant phase element (CPEi) (sf, double layer (dl)) used instead of pure capacitance due to the depressed semicircle, Warburg impedance (Z_w), and intercalation capacitance (C_{int}) [2,3]. Due to the single semicircle observed, the impedance can be ascribed to the combination of the surface film and charge-transfer resistance. The parameter of charge-transfer resistance was much lower for the rGO/Fe_3O_4 NCs hybrid paper (32Ω) compared to pure Fe_3O_4 (75Ω).

Reference

[S1] D. M. Phase, S. Tiwari, R. Prakash, A. Dubey, V. G. Sathe, R. J. Choudhary, *J. Appl. Phys*. **2006**.*100*, 123703.

[S2] M. V. Reddy, T. Yu, C. H. Sow, Z. X. Shen, C. T. Lim, G. V. S. Rao, B. V. R. Chowdari, *Adv. Funct. Mater*. **2007**, *17*, 2792.

[S3] M. V. Reddy, S. Madhavi, G. V. S. Rao, B. V. R. Chowdari, *J. Power Sources*. **2006**, *162*, 1312.